Article

Not peer-reviewed version

Silicon Combined with Activated Carbon Enhances Salt Tolerance in Strawberry (*Fragaria × ananassa*) by Reinforcing Ion–Redox Homeostasis and Reshaping the Rhizosphere Microbiome

Chendong Sun *, Zhaoxin Ge, Xiaofang Yang, Xiaobo Xie, Xinyi Liang, Lan Shen, Jianjie Ren, Yuchao Zhang *

Posted Date: 27 February 2026

doi: 10.20944/preprints202602.1825.v1

Keywords: *Fragaria × ananassa*; soluble silicon; activated carbon; rhizosphere microbiome; ion–redox homeostasis

 doi:10.20944/preprints202602.1825.v1

Article

Silicon Combined with Activated Carbon Enhances Salt Tolerance in Strawberry (*Fragaria* × *ananassa*) by Reinforcing Ion–Redox Homeostasis and Reshaping the Rhizosphere Microbiome

Chendong Sun [1,*,†], Zhaoxin Ge [1,2,†], Xiaofang Yang [1], Xiaobo Xie [1], Xinyi Liang [1], Lan Shen [3], Jianjie Ren [4] and Yuchao Zhang [1,*]

[1] The Institute of Horticulture, Zhejiang Academy of Agricultural Sciences, Hangzhou, Zhejiang, China
[2] School of Ecological Technology and Engineering, Shanghai Institute of Technology, Shanghai, China
[3] Institute of Biotechnology, Ningbo Academy of Agricultural Sciences, Ningbo, China
[4] Agricultural and Rural Affairs Bureau of Shangyu District, Shaoxing, Zhejiang, China
* Correspondence: 1005509919@qq.com (C.S.); gzhangyc@zaas.ac.cn (Y.Z.)
† These authors have contributed equally to this work and share first authorship.

Abstract

Soil salinity severely constrains strawberry production by disrupting ion homeostasis and provoking oxidative injury. Here, we investigated whether soluble silicon (Si) and activated carbon (AC) act synergistically to enhance salt tolerance in strawberry (*Fragaria* × *ananassa*). Under NaCl stress, plants showed pronounced growth inhibition, increased Na^+ accumulation and a deteriorated K^+/Na^+ balance, accompanied by elevated reactive oxygen species (ROS) and lipid peroxidation. In contrast, combined Si and AC treatment consistently provided the strongest protection, improving seedling vigor and survival, limiting Na^+ build-up while maintaining a higher K^+/Na^+ ratio, and attenuating oxidative damage as reflected by reduced ROS and MDA levels together with enhanced activities of antioxidant enzymes (SOD, POD and CAT). Beyond plant responses, AC-containing treatments alleviated salt-induced increases in soil electrical conductivity and improved soil nutrient availability, coinciding with a clear restructuring of the rhizosphere bacterial community and enrichment of putatively beneficial taxa. Transcriptome profiling further supported coordinated reprogramming of ion transport, redox control and stress-responsive signaling pathways under the Si+AC regime. Collectively, our results indicate that Si and AC co-application enhances strawberry salt tolerance through an integrated soil–plant–microbiome mechanism that stabilizes ion homeostasis and reinforces redox homeostasis.

Keywords: *Fragaria* × *ananassa*; soluble silicon; activated carbon; rhizosphere microbiome; ion–redox homeostasis

1. Introduction

Soil salinization is expanding across irrigated and coastal agricultural regions and is increasingly recognized as a major constraint on sustainable horticultural production. Salt stress imposes a rapid osmotic phase that limits growth, followed by a slower ionic phase characterized by toxic Na^+ and Cl^- accumulation and accelerated senescence [1–3]. Physiologically, salinity disrupts cellular ion balance, impairs photosynthesis, and triggers oxidative stress through excessive reactive oxygen species (ROS) formation, ultimately constraining biomass accumulation and yield [1–3]. Because salinity tolerance is a complex trait integrating growth, water relations, ion homeostasis, and stress physiology, carefully designed phenotyping and appropriate physiological indices are essential to interpret treatment effects and to identify causal traits [3].

 doi:10.20944/preprints202602.1825.v1

At the mechanistic level, maintenance of low cytosolic Na^+ and adequate K^+ is central to salinity tolerance. Plants restrict Na^+ entry, extrude Na^+ from the cytosol, retrieve Na^+ from the xylem stream, and compartmentalize Na^+ in vacuoles to reduce cytotoxicity [1,2]. These ion-transport processes are embedded within broader stress signaling networks that coordinate ion and water transport, metabolic adjustment, and gene-expression reprogramming under stress [2]. In parallel, ROS homeostasis and antioxidant defenses play pivotal roles in limiting membrane damage and maintaining cellular stability during salt exposure, interacting with hormonal and transcriptional programs that shape whole-plant outcomes [2,4]. As a result, practical salt-mitigation strategies that can consistently improve plant performance often converge on two axes: improved Na^+/K^+ homeostasis and water status and reinforced redox balance and stress resilience.

Cultivated strawberry (*Fragaria* × *ananassa* Duch.) is generally considered salt-sensitive in production systems, where saline irrigation water or saline soils can markedly compromise plant vigor and productivity [5–8]. Although the molecular basis of strawberry salt responses is still being refined, transcriptome-level evidence indicates that osmotic stresses (including salinity) reshape stress-response pathways and antioxidant-related processes in strawberry tissues, highlighting the relevance of ion–redox coordination for performance under stress [9]. However, bridging these molecular signatures to tractable, root-zone interventions remains challenging. In particular, strawberry is grown in diverse substrates and soil-management regimes where rhizosphere physicochemistry and microbial communities can strongly modulate stress responses, making it important to evaluate salt-mitigation approaches through an integrated plant–soil–microbiome framework.

Among agronomically feasible interventions, silicon (Si) is widely studied as a beneficial element that can enhance tolerance to abiotic stresses, including salinity. Reviews synthesizing multi-species evidence indicate that Si often improves plant water status and salinity performance through multiple, context-dependent mechanisms, including reduced Na^+ uptake/translocation, improved K^+ nutrition, enhanced antioxidant capacity, and altered stress-responsive gene expression [10,11]. Mechanistic models further propose that Si-mediated improvements in water relations can involve coordinated regulation of aquaporins and root hydraulic conductance under salinity, thereby supporting water uptake during osmotic stress [12]. Consistent with this concept, experimental evidence in cucumber demonstrates that Si supply can mitigate salt-induced declines in root hydraulic conductivity and upregulate root aquaporin gene expression, improving water uptake and overall salt tolerance even when changes in shoot Na^+ may be modest or genotype-dependent [13]. Collectively, these data support Si as a practical lever to enhance the water–ion axis of salt tolerance, while emphasizing the need to define effective Si forms and regimes for specific crops and production settings.

In parallel, carbon-based soil amendments—most prominently biochar—have attracted attention for improving soil physical–chemical properties and promoting plant performance under drought and salt stress. A comprehensive review indicates that biochar can alleviate salt stress by improving soil water-holding capacity and associated soil functions and by influencing plant ion relations (often reducing Na^+ uptake while supporting K^+ uptake), stomatal behavior, and phytohormonal regulation, although outcomes depend on biochar type and application rate [14]. Beyond abiotic stress mitigation, biochar can reshape soil microbial communities and has been reviewed as a contributor to pathogen suppression and induced plant defenses through changes in soil properties, root exudation, and microbial ecology [15]. These features are conceptually relevant to activated carbon–like materials as well, because high surface area and sorptive properties can alter nutrient/ion availability and create microhabitats that influence microbial assembly in the rhizosphere.

The rhizosphere microbiome is now recognized as a major determinant of plant performance, including stress tolerance. Foundational reviews highlight that plants shape their rhizosphere microbiome and that the root-associated microbiome can enhance plant health and productivity [16,17]. Work across crop systems supports a multistep model for root microbiome assembly, with

 doi:10.20944/preprints202602.1825.v1

strong compartmentalization among rhizosphere, rhizoplane, and endosphere communities and sensitivity to soil source and cultivation practices [17]. At the mechanistic interface, beneficial microbes can induce systemic resistance and prime plant defense pathways, improving resilience with relatively low fitness costs under non-stress conditions [18]. Thus, management practices that shift rhizosphere communities toward beneficial consortia may provide durable leverage for stress mitigation.

A particularly relevant class of beneficial microbes are plant growth-promoting bacteria (PGPB), which can enhance plant performance under salinity and drought through multiple mechanisms. Reviews emphasize that PGPB can modulate plant hormone balance, improve nutrient acquisition, produce osmoprotective compounds, reinforce antioxidant defenses, and suppress pathogens—functions that are often especially valuable under abiotic stress [19–21]. Among these mechanisms, bacterial ACC deaminase has been extensively discussed as a stress-modulating trait: by lowering plant ACC (the ethylene precursor), ACC deaminase-positive bacteria can reduce stress-induced ethylene accumulation and associated growth inhibition, contributing to improved tolerance under salinity and other stresses [22–25]. Accordingly, strategies that enrich or introduce beneficial bacteria with such traits may complement mineral and soil amendments targeting the water–ion axis.

Importantly, recent synthesis points to the potential complementarity of combining biochar with PGPB, reporting that co-application often yields greater improvements in crop performance than either input alone and proposing mechanistic bases for positive interactions between biochar-mediated habitat modification and microbial functions [26]. In addition, studies integrating biochar with specific functional microbes show that "microbe-loaded" biochar can enhance soil enzyme activity and reshape microbial community features, illustrating a plausible route by which carbonaceous amendments can act as microbial carriers or ecological filters [27]. These insights support a broader hypothesis for strawberry salt mitigation: combining silicon-based interventions (targeting water relations and ion homeostasis) with carbonaceous amendments (modifying soil properties and microbial assembly) could generate additive or synergistic improvements, potentially mediated through rhizosphere community enrichment and early host stress reprogramming.

Despite the conceptual appeal, evidence remains limited for integrated "Si + carbonaceous amendment" strategies in strawberry under progressive salinity regimens, particularly with multi-layered evaluation linking plant phenotypes to rhizosphere microbiome shifts and ion–redox regulatory signatures. Addressing this gap is timely because saline stress in production systems is often gradual and cumulative, and because strawberry's performance may be especially sensitive to root-zone conditions and microbial interactions. Here, we evaluate whether combining silicon supply with a carbon-based amendment improves strawberry performance under salt stress and whether these benefits align with enrichment of beneficial rhizosphere bacteria and activation of host ion–redox programs, providing a mechanistic framework for practical management in salt-affected cultivation systems.

2. Materials and Methods

2.1. Plant Materials and Growth Conditions

Tissue-cultured strawberry (*Fragaria* × *ananassa* Duch.) plantlets (cv. *Jiandebailu*) were rooted for ~30 d, and uniform plantlets with comparable vigor were selected. Plants were transplanted individually into 6.5 cm plastic pots containing a sterilized substrate mixture of peat:vermiculite:perlite (3:3:1, v/v/v) and cultivated in a plant factory located in Shangyu District, Shaoxing, Zhejiang Province, China. Pots were maintained in a controlled-environment growth chamber under a 12 h light/12 h dark photoperiod with an irradiance of 12,000 lux, and the air temperature was kept constant at 25 °C during both the light and dark periods (25/25 °C, day/night). During acclimation, plants were watered every three days with half-strength Murashige and Skoog solution (1/2 MS).

 doi:10.20944/preprints202602.1825.v1

2.2. Preparation of Activated Carbon-Amended Substrate

Commercial activated carbon (AC; OriLeaf Bio-Technology Co., Ltd., China; product no. W14584) was washed thoroughly with deionized water and oven-dried prior to use. AC was incorporated into the substrate at 2% (w/w, dry weight basis), and the amended substrate was mixed thoroughly and equilibrated for 5 d before microbial inoculation.

2.3. Preparation of Saline–Alkali Soil Microbial Inoculum and Substrate Inoculation

A microbial consortium was enriched from saline–alkali strawberry soil collected in the Dajiangdong area, Qiantang District, Hangzhou, Zhejiang Province, China. Soil suspensions were used to inoculate LB broth and incubated at 28 °C with shaking (180 rpm) for 48 h. Cells were harvested by centrifugation (8000×g, 10 min), washed twice with sterile water, and resuspended to OD600=1.0. The standardized suspension was added to both AC-amended and AC-free substrates, mixed thoroughly to ensure homogeneous inoculation, sealed to maintain moisture, and incubated for 7 d prior to transplanting.

2.4. Experimental Design and Salt/Silicon Treatments

The experiment followed a completely randomized design with five treatments: Control, NaCl, NaCl+Si, NaCl+AC, and NaCl+AC+Si, with 70 pots per treatment (one plant per pot) to accommodate destructive sampling and phenotyping. After a 14-d acclimation period, silicon was supplied as potassium silicate (K_2SiO_3) at 1.5 mM; to control for potassium input, non-silicon treatments received KCl at an equimolar K^+ dose (3 mM KCl). Salt stress was imposed stepwise to minimize osmotic shock by irrigating salt-stressed plants with 1/2 MS containing 60 mM NaCl (Day 15), 100 mM NaCl (Day 16), and 150 mM NaCl (Day 17), while control plants received 1/2 MS without NaCl throughout; excess drainage in trays was promptly removed to avoid unintended bottom soaking.

2.5. Sampling Scheme

The experiment followed a completely randomized design with five treatments (Control, NaCl, NaCl+Si, NaCl+AC, and NaCl+AC+Si), with 70 pots per treatment (one plant per pot) to accommodate destructive sampling and phenotyping. After a 14-d acclimation period, silicon was supplied as potassium silicate (K_2SiO_3) at 1.5 mM; to control for potassium input, non-silicon treatments received KCl at an equimolar K^+ dose (3 mM KCl). Salt stress was imposed stepwise to minimize osmotic shock by irrigating salt-stressed plants with 1/2 MS containing 60 mM NaCl (Day 15), 100 mM NaCl (Day 16), and 150 mM NaCl (Day 17), while control plants received 1/2 MS without NaCl throughout; excess drainage in trays was promptly removed to avoid unintended bottom soaking. For soil physicochemical analyses, substrate was sampled at two time points: (1) after microbial incubation but prior to transplanting, where AC(+) and AC(−) substrates were each sampled in triplicate for EC, pH, and Na/K determinations; and (2) after 7 d at 150 mM NaCl, where substrate from each of the five treatments was collected from three pots per treatment for EC, pH, and Na/K measurements.

2.6. Growth Traits and Survival Assessment

At the endpoint of the salt treatment, shoots and roots were separated and fresh weight was determined on an individual-plant basis (n = 12 plants per treatment). Seedling survival was evaluated under 150 mM NaCl using independent plants (n = 40 plants per treatment) and expressed as survival rate (%). For survival scoring, a plant was considered alive when it retained ≥2 fully expanded green leaves with no visible marginal necrosis, chlorosis, or wilting; plants not meeting this criterion were scored as dead. Fresh-weight data were compared among treatments by one-way analysis of variance followed by Tukey's HSD for multiple comparisons, whereas survival data were analyzed as binomial outcomes using pairwise Fisher's exact tests with Holm correction; statistical implementation and figure generation were performed in R.

 doi:10.20944/preprints202602.1825.v1

2.7. Soil Physicochemical Properties (EC, pH, and Soil Ions)

Soil/substrate samples were collected at two time points: (1) after microbial incubation but prior to transplanting, where AC(+) and AC(−) substrates were each sampled in triplicate; and (2) after 7 d at 150 mM NaCl, where substrate from each of the five treatments was collected (three pots per treatment) for physicochemical analyses. For EC and pH determination, 5 g of fresh substrate was extracted with 25 mL deionized water (1:5, w/v), and EC and pH were measured in the slurry using a portable multiparameter meter (HI98195, Hanna Instruments, USA). Aliquots of the same soil–water extract were clarified (by settling and/or filtration) and analyzed for Na and K using ICP-OES (iCAP Pro X, Thermo Fisher Scientific, USA).

2.8. Determination of Na^+ and K^+ in Plant Tissues

Shoot and root tissues were harvested separately, briefly rinsed with deionized water, and oven-dried at 80 °C to constant weight. Dried samples were ground to a fine powder, and 0.10 g of each sample was wet-digested with concentrated H_2SO_4 using H_2O_2 as an oxidant at 280 °C until the solution became clear. The digests were filtered and brought to a final volume of 50 mL with deionized water, and Na^+ and K^+ concentrations were quantified using ICP-OES (iCAP Pro X, Thermo Fisher Scientific, USA). The K^+/Na^+ ratio was calculated accordingly.

2.9. Oxidative Stress Markers (MDA, H_2O_2, and $O_2\cdot^-$)

At the endpoint of the salt treatment, fresh leaves were collected, immediately frozen in liquid nitrogen, and stored at −80 °C; all assays were completed within 2 weeks. Malondialdehyde (MDA) content was determined using a commercial kit (Suzhou Comin Biotechnology Co., Ltd., China; MDA-1-Y) based on the thiobarbituric acid (TBA) reaction: ~0.1 g tissue was homogenized on ice in 1 mL extraction buffer, centrifuged (8000×g, 4 °C, 10 min), and the supernatant was processed following the manufacturer's protocol; absorbance was recorded at 532 and 600 nm using a microplate reader (Spark®, Tecan, Switzerland). Superoxide anion ($O_2\cdot^-$) level/production rate was quantified with a hydroxylamine-based kit (Suzhou Comin Biotechnology Co., Ltd., China; SA-1-G); ~0.1 g tissue was extracted on ice in 1 mL extraction buffer, centrifuged (10,000×g, 4 °C, 20 min), and absorbance was measured at 530 nm. Hydrogen peroxide (H_2O_2) content was determined using a titanium sulfate microplate kit (Beijing Leagene Biotechnology Co., Ltd., China; TO1075) and read at 412 nm (Spark®, Tecan), all according to the manufacturers' instructions.

2.10. Rhizosphere Microbiome Sampling, 16S rRNA Sequencing, and Bioinformatics

Rhizosphere samples were collected after 7 d of 150 mM NaCl treatment by gently removing loosely attached substrate, followed by resuspension of tightly adhering rhizosphere soil in sterile water and centrifugation to obtain a rhizosphere pellet for downstream DNA-based analyses. Genomic DNA extraction, PCR amplification, library construction, Illumina sequencing, and primary bioinformatics were performed by Shanghai Majorbio Bio-pharm Technology Co., Ltd. (Shanghai, China). Briefly, bacterial 16S rRNA gene amplicons were generated using a two-step PCR strategy with two primer sets (first round: 799F/1392R; second round: 799F/1193R); primer sequences were 799F (AACMGGATTAGATACCCKG) and 1193R (ACGTCATCCCCACCTTCC), and PCR was conducted with an annealing temperature of 55 °C and a unified cycle number across samples for the formal amplification (13 cycles in the second round). Libraries were sequenced on an Illumina NextSeq 2000 platform in paired-end mode (PE300). Amplicon reads were processed to generate amplicon sequence variants (ASVs) using QIIME 2 with DADA2 denoising (including quality control and chimera removal), and taxonomic assignment was performed against the SILVA database [28–30]. The resulting ASV table and taxonomy annotations were subsequently analyzed in R, including alpha diversity estimation, Bray–Curtis dissimilarity-based ordination and PERMANOVA, and differential abundance testing using ANCOM-BC with false discovery rate control [31,32]. Raw

 doi:10.20944/preprints202602.1825.v1

sequencing reads have been deposited in the NCBI Sequence Read Archive under BioProject accession PRJNA1424400.

2.11. RNA Extraction, Library Construction, RNA-Seq Data Processing, and Heatmap Visualization

For transcriptome profiling, total RNA was extracted from treated strawberry tissues using TRIzol® reagent following the manufacturer's instructions, quantified spectrophotometrically, and assessed for integrity using an Agilent Bioanalyzer; only high-quality RNA was used for subsequent library construction. RNA purification, strand-specific mRNA library preparation and Illumina sequencing were performed by Shanghai Majorbio Bio-pharm Technology Co., Ltd. (Shanghai, China), including poly(A)$^+$ mRNA enrichment, fragmentation, cDNA synthesis, end repair, adapter ligation, size selection, and PCR enrichment. After adapter trimming and quality filtering with fastp [33], clean reads were aligned to the octoploid cultivated strawberry (*Fragaria* × *ananassa*) 'Benihoppe' reference genome [34] using HISAT2 [35] with strand-specific settings (RF), and the resulting alignments were processed with SAMtools [36]. Reference-guided transcript assembly and quantification were carried out using StringTie [37], and gene-level count matrices were generated for downstream differential expression analysis in DESeq2 with Benjamini–Hochberg false discovery rate control [38]. The Gene Ontology (GO) and Kyoto Encyclopedia of Genes and Genomes (KEGG) annotations for strawberry genes were performed using the online software EggNOG-Mapper (http://eggnog-mapper.embl.de/), while GO and KEGG enrichment analyses were performed using Tbtools software [39]. For visualization of selected genes, heatmaps were generated in R using the pheatmap package based on $\log_2$ (*FPKM* + 1)–transformed expression values; to facilitate cross-treatment comparison, expression values were centered per gene by subtracting the corresponding Control mean (thereby displaying relative changes from Control), with hierarchical clustering applied to genes and sample columns arranged according to the experimental design. Raw sequencing reads have been deposited in the NCBI Sequence Read Archive under BioProject accession PRJNA1424399.

2.12. Statistical Analysis

All statistical analyses and figure generation were conducted in R (R Foundation for Statistical Computing, Vienna, Austria). Survival rate (binary outcome) was analyzed using pairwise Fisher's exact tests with Holm adjustment for multiple comparisons, and 95% binomial confidence intervals were calculated; significance groupings were displayed as compact letter displays. For continuous traits (fresh weight, H_2O_2, MDA, $O_2^{\cdot-}$, plant Na^+/K^+ and Na^+/K^+ ratio, soil EC/pH, and soil Na^+/K^+), treatment effects were evaluated by one-way ANOVA followed by Tukey's HSD for all-pair comparisons, and Dunnett-type comparisons versus the Control were additionally reported where applicable [40]. Rhizosphere microbiome community analyses were performed in R from the processed ASV table, including alpha diversity estimation, Bray–Curtis dissimilarity-based ordination, and PERMANOVA (vegan), while differential abundance testing was performed using ANCOM-BC2 with false discovery rate control [32]. In all analyses, differences were considered significant at $p < 0.05$.

3. Results

3.1. Co-Application of Activated Carbon and Silicon Mitigated Salt Injury and Improved Plant Performance

The experimental design, treatment regime, and sampling workflow are summarized in **(Figure S1)**. Under severe salinity (150 mM sodium chloride, NaCl), strawberry seedlings exhibited pronounced injury symptoms compared with the non-saline control **(Figure 1A)**. NaCl markedly reduced survival, whereas the combined treatment with activated carbon (AC) and silicon (Si; supplied as potassium silicate, K_2SiO_3) improved survival relative to NaCl alone; single amendments (Si or AC) showed weaker benefits **(Figure 1B)**. Consistently, salt stress substantially decreased shoot and root fresh weights, and Si+AC partially restored biomass among salt-stressed plants **(Figure 1C,D)**.

 doi:10.20944/preprints202602.1825.v1

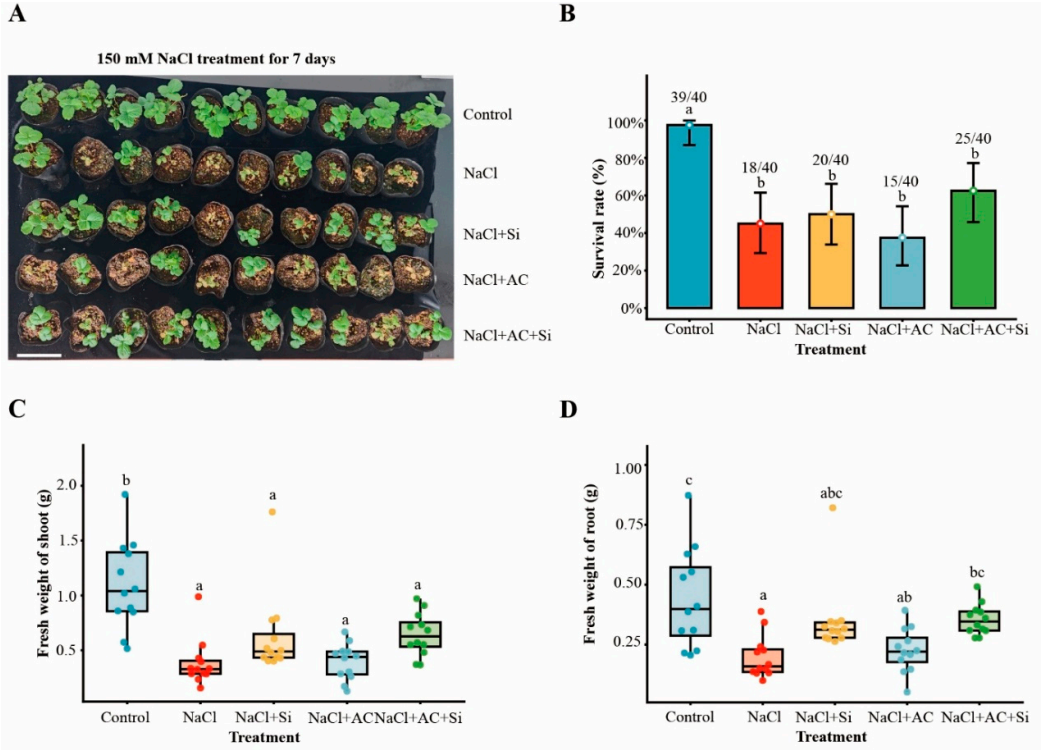

Figure 1. Effects of activated carbon (AC) and silicon (Si; supplied as potassium silicate, K_2SiO_3) on strawberry plant performance under salt stress. (A) Representative phenotypes after 150 mM NaCl treatment (10 d) under the indicated treatments. The white line segment indicates a scale bar of 6 cm. (B) Survival rate after 150 mM NaCl (10 d). Numbers above bars indicate surviving plants/total plants. Error bars represent 95% binomial confidence intervals. Survival (binary outcome) was analyzed using pairwise Fisher's exact tests with Holm adjustment for multiple comparisons; significance groupings are displayed as compact letter displays. Different letters indicate significant differences at $P < 0.05$. (C) Shoot fresh weight. (D) Root fresh weight. Continuous traits were evaluated by one-way analysis of variance (ANOVA) followed by Tukey's honestly significant difference (HSD) test for all-pair comparisons; Dunnett-type comparisons versus the Control were additionally reported where applicable. Different letters indicate significant differences at $P < 0.05$.

3.2. AC+Si Modulated Soil Properties and Reshaped Rhizosphere Bacterial Communities Under Salinity

Soil electrical conductivity (EC) increased strongly under NaCl, confirming successful establishment of salinity stress; among salt treatments, the Si+AC group showed comparatively lower EC than the other NaCl-containing treatments (**Figure 2A**). Soil pH varied within a narrow range across treatments (**Figure 2B**). Soil Na^+ content increased sharply under salinity and was broadly comparable among the salt-treated groups (**Figure 2C**), whereas soil K^+ differed among treatments and tended to be higher in the Si-containing treatment (**Figure 2D**). For rhizosphere bacterial profiling, sequencing depth and basic quality metrics indicated adequate coverage across samples **(Table S1)**. Community structure differed clearly among treatments, as shown by Bray–Curtis principal coordinates analysis (PCoA) **(Figure 2E)**. Differential abundance analysis revealed that comparisons involving Si+AC yielded the greatest number of significantly shifted genera **(Figure 2F)**. In particular, Si+AC differed from NaCl and from NaCl+AC with multiple genera showing significant shifts, including signals involving *Pseudomonas* and *Neorhizobium* **(Figure 2G,H; Table S2)**. Alpha-diversity indices and genus-level composition profiles further supported treatment-associated restructuring of rhizosphere bacterial assemblages **(Figure S2A–C)**.

 doi:10.20944/preprints202602.1825.v1

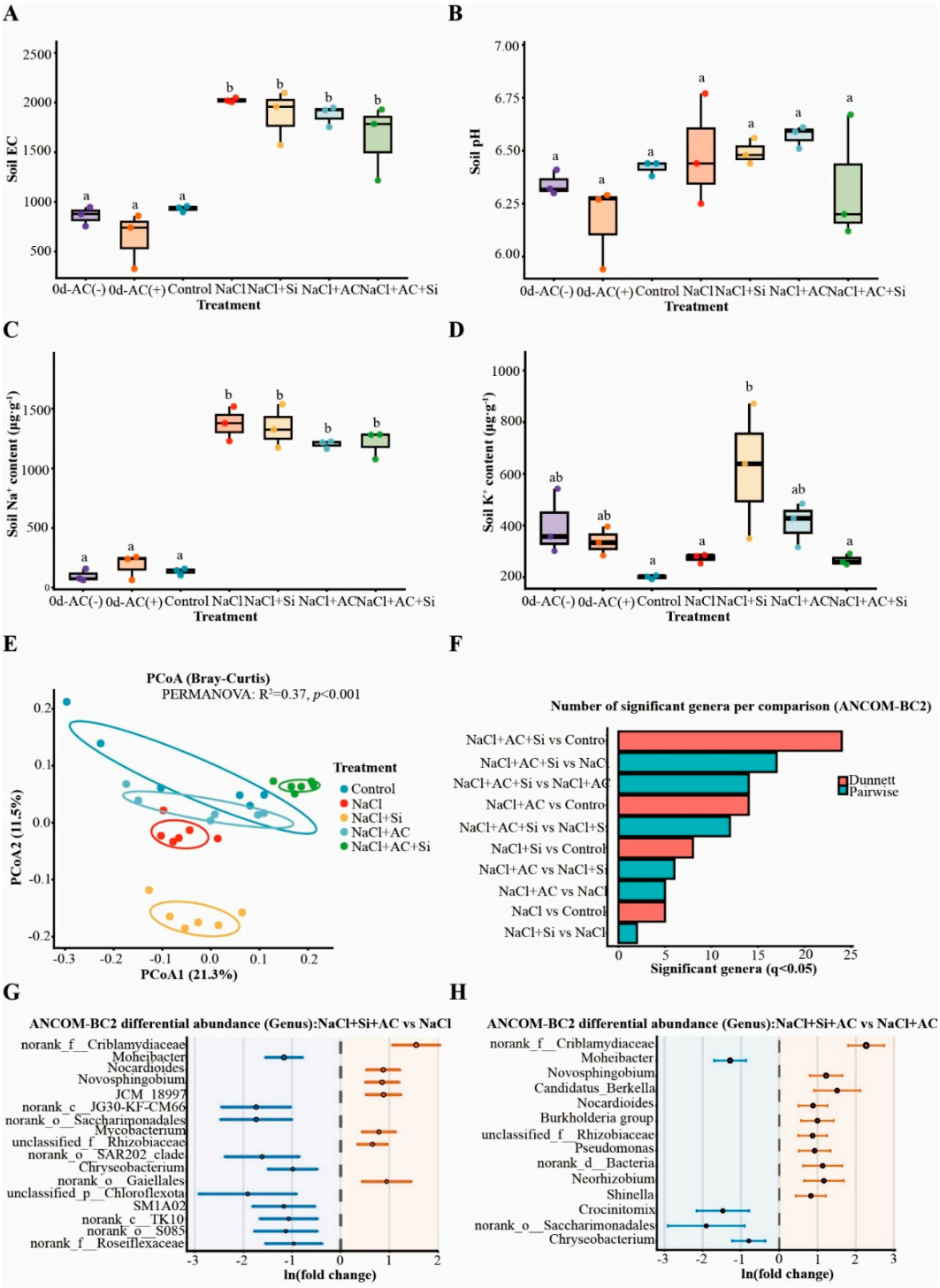

Figure 2. Effects of AC and Si on soil physicochemical properties and rhizosphere bacterial community composition. (A) Soil electrical conductivity (EC). (B) Soil pH. (C) Soil Na^+ content. (D) Soil K^+ content. "0 d-AC(−)" and "0 d-AC(+)" indicate baseline soils before planting under AC-free and AC-amended conditions, respectively. Soil traits were analyzed by one-way ANOVA followed by Tukey's HSD; Dunnett-type comparisons versus the Control were additionally reported where applicable. Different letters indicate significant differences at $P < 0.05$. (E) Principal coordinates analysis (PCoA) based on Bray–Curtis dissimilarity of rhizosphere bacterial communities; permutational multivariate analysis of variance (PERMANOVA; vegan) statistics are shown in the panel. (F) Number of significantly differential genera per comparison identified by ANCOM-BC2 with false discovery rate control; significance threshold $q < 0.05$. (G–H) Genus-level differential

 doi:10.20944/preprints202602.1825.v1

abundance (ANCOM-BC2) for NaCl+Si+AC vs NaCl (G) and NaCl+Si+AC vs NaCl+AC (H), presented as ln(fold change) with confidence intervals; full outputs are provided in Table S2. In panel H, the sixth taxon label "Burkholderia–Caballeronia–Paraburkholderia" is a condensed/combined genus annotation (Burkholderia sensu lato complex) commonly used in 16S genus-level reporting to represent closely related genera that may not be reliably separated at this marker resolution.

3.3. AC+Si Improved Ion Homeostasis Primarily by Reducing Shoot Na^+ Accumulation and Lowering the Shoot Na^+/K^+ Ratio

Salt stress induced strong Na^+ accumulation in both roots and shoots **(Figure 3A,B)** and altered K^+ status relative to the control **(Figure 3C,D)**. Notably, the combined Si+AC treatment reduced shoot Na^+ relative to NaCl and the single-amendment treatments **(Figure 3B)**. Na^+/K^+ ratios increased substantially under salinity in both roots and shoots **(Figure 3E,F)**, whereas Si+AC produced the most consistent reduction of the shoot Na^+/K^+ ratio among salt-treated plants **(Figure 3F)**, indicating improved ionic balance in aboveground tissues.

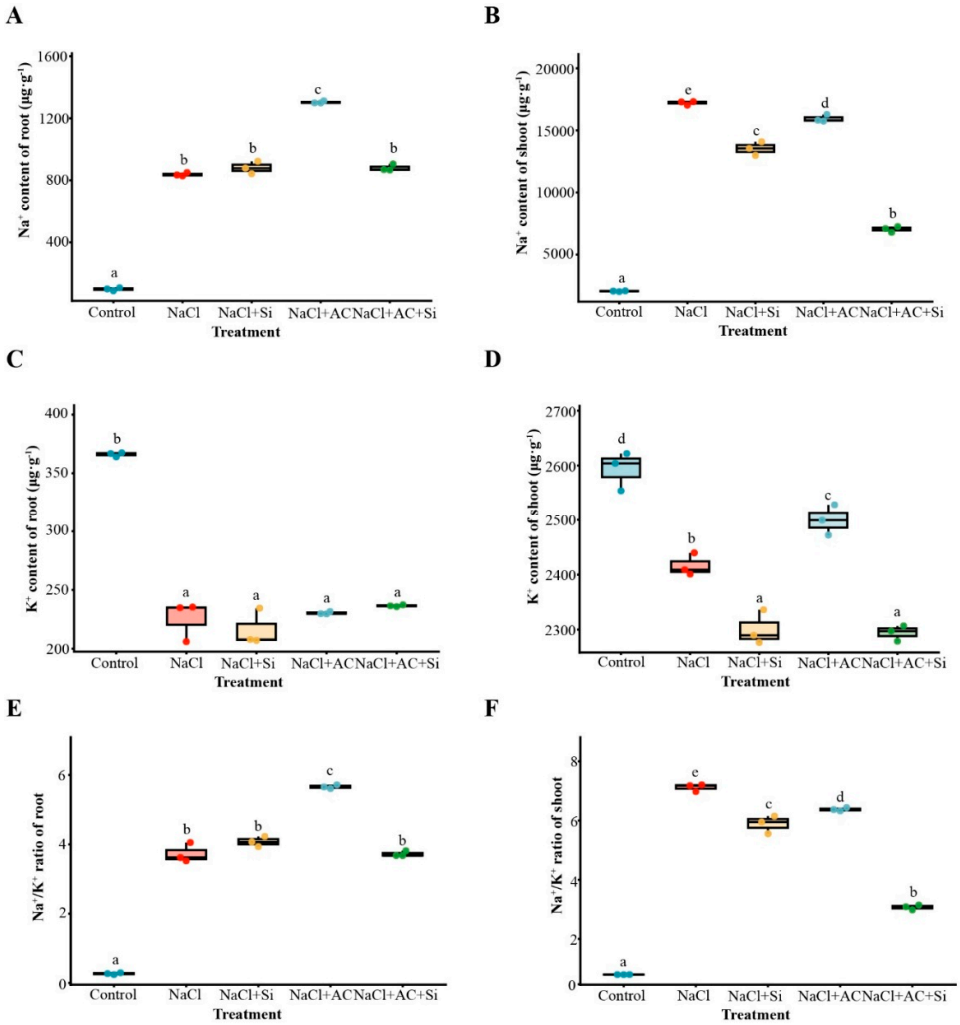

Figure 3. Effects of AC and Si on ion homeostasis in strawberry plants under salt stress. (A) Root Na^+ content. (B) Shoot Na^+ content. (C) Root K^+ content. (D) Shoot K^+ content. (E) Root Na^+/K^+ ratio. (F) Shoot Na^+/K^+ ratio. Continuous traits were analyzed by one-way ANOVA followed by Tukey's HSD; Dunnett-type comparisons versus the Control were additionally reported where applicable. Different letters indicate significant differences at $P < 0.05$.

 doi:10.20944/preprints202602.1825.v1

3.4. AC+Si Attenuated Salt-Induced Oxidative Damage in Roots and Shoots

Salt stress markedly increased oxidative stress indicators. $O_2\cdot^-$ production rates rose in both roots and shoots under NaCl, whereas Si+AC reduced $O_2\cdot^-$ among salt-treated plants **(Figure 4A,B)**. H_2O_2 content similarly increased under NaCl and was reduced under Si+AC in both tissues, with a clearer attenuation in roots **(Figure 4C,D)**. Lipid peroxidation, reflected by malondialdehyde (MDA) accumulation, was enhanced by salinity and was comparatively lower under Si+AC among the salt treatments **(Figure 4E,F)**, supporting reduced oxidative injury under the combined amendment.

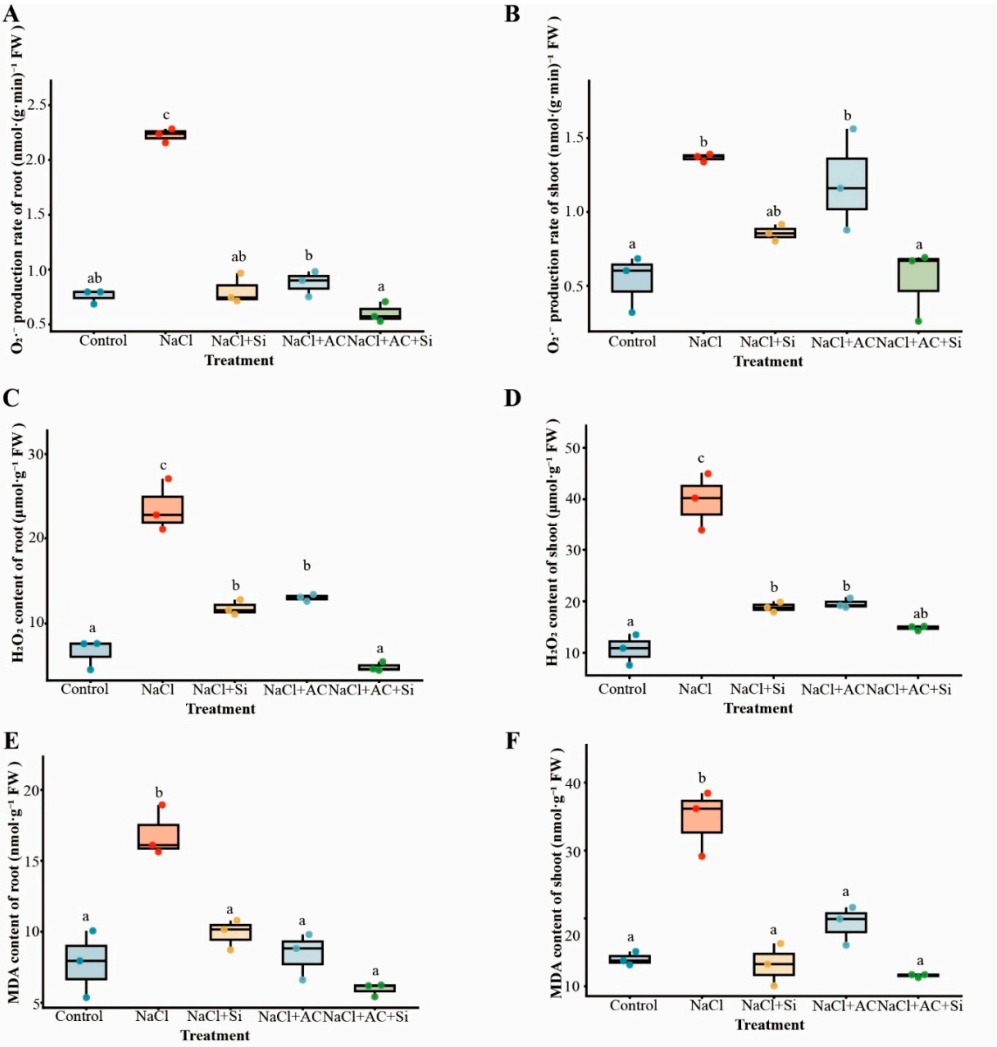

Figure 4. Effects of AC and Si on oxidative stress markers in strawberry plants under salt stress. (A) Root $O_2\cdot^-$ production rate. (B) Shoot $O_2\cdot^-$ production rate. (C) Root H_2O_2 content. (D) Shoot H_2O_2 content. (E) Root MDA content. (F) Shoot MDA content. Continuous traits were analyzed by one-way ANOVA followed by Tukey's HSD; Dunnett-type comparisons versus the Control were additionally reported where applicable. Different letters indicate significant differences at $P < 0.05$.

3.5. Transcriptome Profiling Supported Coordinated Induction of Ion-Transport and Redox/ROS-Mitigation Programs Under AC+Si

RNA sequencing (RNA-seq) data showed clear treatment separation and strong replicate concordance **(Figure 5A; Figure S3)**. Relative to NaCl, Si+AC induced a distinct subset of upregulated genes while sharing a substantial fraction of induced genes with the single-amendment treatments **(Figure 5B)**. Gene Ontology (GO) enrichment of Si+AC-specific induced genes highlighted stimulus-response and

 doi:10.20944/preprints202602.1825.v1

redox-related functions **(Figure 5C)**, while Kyoto Encyclopedia of Genes and Genomes (KEGG) enrichment indicated involvement of transport- and metabolism-associated categories **(Figure 5D)**. Importantly, the heatmap of curated Si+AC-responsive candidate genes showed a coherent expression pattern across biological replicates: compared with NaCl, many candidates annotated to ion transport and redox/reactive oxygen species (ROS) detoxification displayed higher expression under Si+AC, accompanied by coordinated changes in genes linked to cell wall/defense-related processes **(Figure 5E; Table S3)**. Collectively, these transcriptomic signatures are consistent with the physiological improvements in ion balance and oxidative stress mitigation observed under the combined treatment.

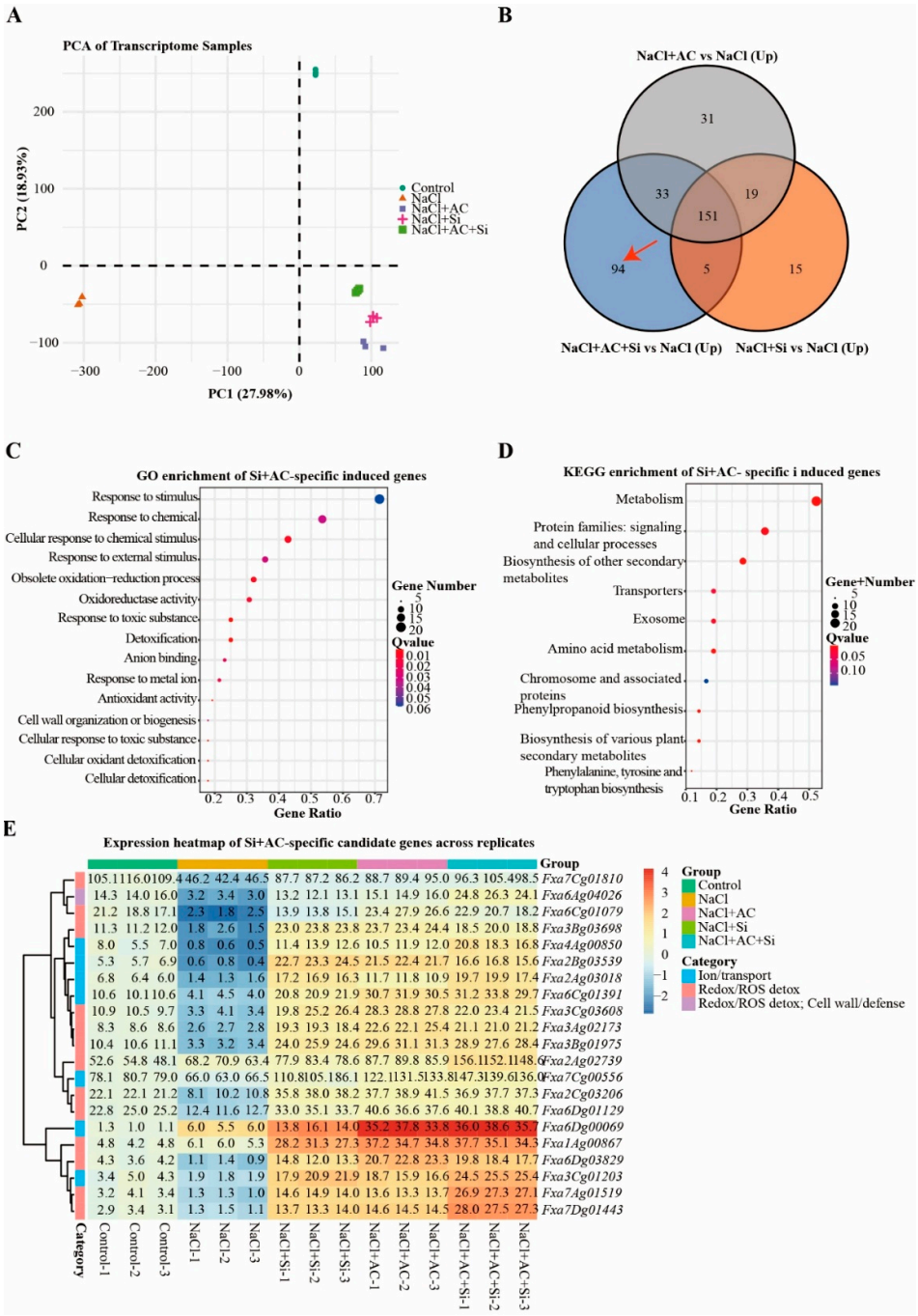

Figure 5. Transcriptome analysis of strawberry plants under different treatments. (A) Principal component analysis (PCA) of transcriptome samples. (B) Venn diagram of upregulated genes in NaCl+Si vs NaCl, NaCl+AC

 doi:10.20944/preprints202602.1825.v1

vs NaCl, and NaCl+Si+AC vs NaCl. Differentially expressed genes (DEGs) were identified using the criteria fold change ≥ 2 (+|log2FC| ≥ 1) and P < 0.01. (C) Gene Ontology (GO) enrichment of Si+AC-specific induced genes. (D) KEGG enrichment of Si+AC-specific induced genes. (E) Heatmap showing expression of Si+AC-specific candidate genes across biological replicates. Expression values are shown as log_2(FPKM + 1) and row-centered by subtracting the mean of the Control group; functional categories are indicated. The curated candidate gene list is provided in Table S3.

4. Discussion

Salt stress limits strawberry growth through a rapid osmotic phase and a slower ionic phase, the latter marked by Na^+ over-accumulation, impaired K^+ nutrition, and secondary oxidative injury [1,41,42]. Across our assays, potassium silicate (Si source) and activated carbon (AC) did not contribute equally: Si alone showed partial protection, AC alone provided little benefit, whereas their co-application produced the most consistent improvements in plant performance, ion balance, redox status, rhizosphere community structure, and stress-responsive transcription (**Figure 1–5; Figure S1–S3; Table S1**). Collectively, the data support synergy rather than simple additivity (**Figure 6**).

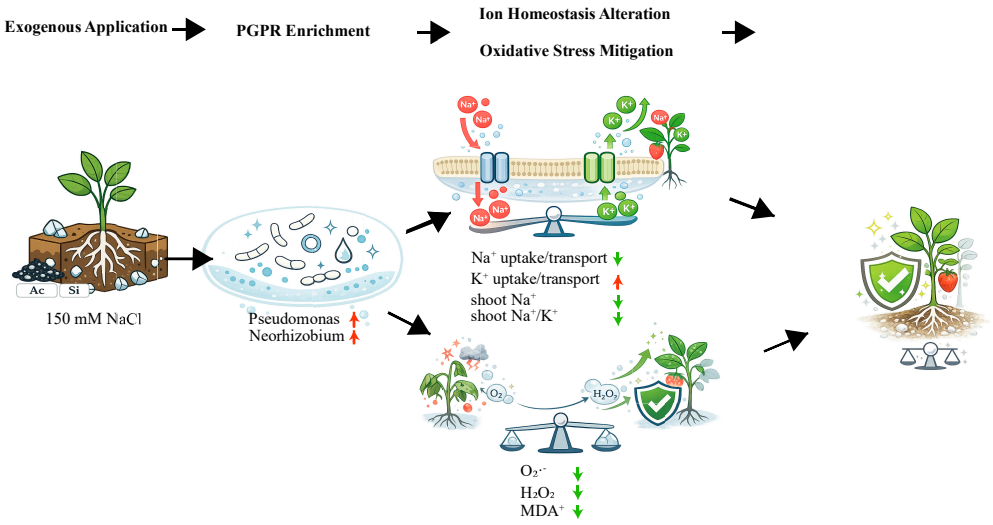

Figure 6. Proposed working model for the synergistic alleviation of salt stress by AC and Si in strawberry. Conceptual model summarizing that AC+Si reshapes rhizosphere bacterial communities and improves host ion homeostasis and oxidative stress mitigation, collectively alleviating salt stress symptoms.

4.1. A Non-Additive Response: Si Helps, AC Alone Is Weak, and Si+AC Is Most Effective

In many crops, silicon acts as a beneficial element rather than an essential nutrient, yet it frequently mitigates salinity damage by improving root function, strengthening apoplastic barriers, modulating transport processes, and supporting antioxidant capacity [43–45]. Your data fit this general framework: silicate application alone improved salt tolerance but did not fully restore growth under severe salinity, while AC alone did not reproducibly increase tolerance (**Figure 1**). A plausible interpretation is that AC primarily alters the root-zone context (sorption, nutrient and metabolite availability, and microhabitat structure) rather than directly triggering plant stress tolerance. Carbonaceous amendments can therefore yield variable plant outcomes depending on material properties and soil–plant conditions [14,46]. When combined, Si and AC likely act through complementary routes—Si supporting plant physiological buffering and AC reshaping the rhizosphere environment—leading to a response that is better described as synergistic than additive (**Figure 6**).

 doi:10.20944/preprints202602.1825.v1

4.2. Ion Homeostasis and Redox Buffering: A Coherent Physiological Explanation

Maintaining low cytosolic Na^+ and adequate K^+ is central to salt tolerance, because K^+ is required for enzyme activity, protein synthesis, and membrane potential maintenance [1,41,42]. In this study, the combined treatment produced the most favorable ion phenotype under NaCl, improving Na^+/K^+ status relative to NaCl alone (**Figure 3**). This pattern is consistent with stronger restriction of Na^+ accumulation and/or improved K^+ retention—processes often linked to silicon-mediated changes in root properties and transport regulation [43–45]. Ion imbalance commonly amplifies ROS production and lipid peroxidation, so improvements in ionic homeostasis are expected to translate into reduced oxidative injury [47–49]. Accordingly, oxidative markers shifted in a protective direction under the combined treatment (**Figure 4**), aligning with established roles of ROS–antioxidant networks in abiotic stress responses [47–49]. Taken together, the coordinated improvements in ion homeostasis (**Figure 3**) and redox balance (**Figure 4**) provide a direct physiological explanation for the better survival and biomass under Si+AC (**Figure 1**).

4.3. Rhizosphere Restructuring as an "Amplifier" of Plant Stress Tolerance

Plants actively shape their rhizosphere microbiome, and microbial community shifts can feed back on nutrition, hormone homeostasis, and stress acclimation [16,50]. Rhizosphere profiles here show clear treatment-associated restructuring (**Figure 2E; Figure S2**) and differential enrichment/depletion of specific bacterial genera under Si+AC (**Figure 2F–H**). Although 16S rRNA data cannot establish function at strain resolution, the direction of these shifts is compatible with a microbiome-assisted tolerance model, in which a more favorable rhizosphere community supports plant ion and redox homeostasis during salt stress (**Figure 2–4; Figure 6**). This interpretation is consistent with known mechanisms of plant growth–promoting bacteria, including improved nutrient acquisition and stress modulation via ACC deaminase–mediated attenuation of stress ethylene [23,51,52]. In this context, the limited benefit of AC alone (**Figure 1**) becomes less surprising: carbon sorbents may not consistently enrich a helpful community under severe salinity unless the host plant is simultaneously buffered (here by Si) to sustain productive root exudation and microbial recruitment. Carbon amendments are well known to produce context-dependent outcomes because their sorption behavior can shift nutrient and signaling availability [14,46].

4.4. Transcriptome Insights and Agronomic Relevance

The transcriptome results provide independent support for the coordinated Si+AC response. Samples separated by treatment (**Figure 5A; Figure S3**), and the combined treatment displayed distinct expression patterns and functional themes (**Figure 5B–D**). Importantly, the candidate-gene heatmap indicates that, relative to NaCl alone, Si+AC induced a broad set of genes associated with ion transport/compartmentation and oxidative stress mitigation (**Figure 5E; Table S1**), matching the physiological phenotypes (**Figure 3–4**). From an applied standpoint, amendment-based strategies are attractive for horticulture facing salinization, but effectiveness depends on both plant physiology and the soil–microbiome context. These data suggest that potassium silicate and activated carbon are most effective when applied together in octoploid strawberry (**Figure 1–5**). Key limitations are that (1) controlled-environment results require validation under production-like substrates/field conditions, (2) 16S profiles provide compositional rather than functional proof, and (3) AC performance is material- and dose-dependent. Future work combining isolate/synthetic-community tests with optimized material characterization would help establish causality and guide agronomic deployment [16,23,50–52].

5. Conclusions

NaCl stress markedly impaired seedling performance in octoploid cultivated strawberry (*Fragaria* × *ananassa*), coinciding with soil salinization, disrupted Na^+/K^+ homeostasis, oxidative injury, and rhizosphere community shifts. Against this stress background, the co-application of

 doi:10.20944/preprints202602.1825.v1

potassium silicate and activated carbon provided the most consistent protection, improving growth and survival, enhancing Na^+/K^+ balance, and alleviating oxidative damage (**Figure 1**, **Figure 3–4**). This combined treatment was also associated with altered soil physicochemical properties and rhizosphere bacterial assemblages (**Figure 2**, **Figure S2**, **Table S1**), while transcriptome profiling supported coordinated activation of ion transport- and redox-related pathways (**Figure 5**, **Figure S3**). Together, these findings support a synergistic soil–plant–microbiome mechanism and suggest that co-applying silicate and activated carbon is a promising strategy to mitigate salt stress in strawberry.

Supplementary Materials: The following supporting information can be downloaded at the website of this paper posted on Preprints.org.

Author: Contributions Conceptualization, **C.S.**; methodology, **C.S.**; investigation, **C.S., Z.G., X.L.**; data curation, **C.S., X.Y.**; formal analysis, **C.S., X.X.**; visualization, **C.S.**; writing—original draft preparation, **C.S., Z.G.**; writing—review and editing, **C.S., Y.Z.**; supervision, **Y.Z.**; funding acquisition, **Y.Z., L.S., J.R**. All authors have read and agreed to the published version of the manuscript.

Data: Availability Statement The RNA-seq raw sequencing data generated in this study have been deposited in the NCBI Sequence Read Archive (SRA) under BioProject accession PRJNA1424399. The rhizosphere 16S rRNA amplicon sequencing raw reads have been deposited in the NCBI SRA under BioProject accession PRJNA1424400.

Acknowledgments: This work was supported by the Major Science and Technology Program for Crop New Variety Breeding of Zhejiang Province (No. 2021C02066-7); the Local Science and Technology Cooperation Project of Zhejiang Academy of Agricultural Sciences (No. SY202304); the Zhejiang Provincial Team Science and Technology Commissioner Partner-Service Program; the Zhejiang "Sannong Jiufang" Science and Technology Collaboration Program (No. 2025SNJF029); and the Ningbo Municipal Major Special Project (No. 2023Z112).

Conflicts: of Interest The authors declare no conflict of interest.

References

1. Munns, R.; Tester, M. Mechanisms of salinity tolerance. *Annu Rev Plant Biol* **2008**, *59*, 651-681, doi:10.1146/annurev.arplant.59.032607.092911.
2. Zhu, J.K. Abiotic Stress Signaling and Responses in Plants. *Cell* **2016**, *167*, 313-324, doi:10.1016/j.cell.2016.08.029.
3. Negrao, S.; Schmockel, S.M.; Tester, M. Evaluating physiological responses of plants to salinity stress. *Ann Bot* **2017**, *119*, 1-11, doi:10.1093/aob/mcw191.
4. Zhang, H.; Zhu, J.; Gong, Z.; Zhu, J.K. Abiotic stress responses in plants. *Nat Rev Genet* **2022**, *23*, 104-119, doi:10.1038/s41576-021-00413-0.
5. Li, S.; Chang, L.; Sun, R.; Dong, J.; Zhong, C.; Gao, Y.; Zhang, H.; Wei, L.; Wei, Y.; Zhang, Y.; et al. Combined transcriptomic and metabolomic analysis reveals a role for adenosine triphosphate-binding cassette transporters and cell wall remodeling in response to salt stress in strawberry. *Front Plant Sci* **2022**, *13*, 996765, doi:10.3389/fpls.2022.996765.
6. Zahedi, S.M.; Abdelrahman, M.; Hosseini, M.S.; Hoveizeh, N.F.; Tran, L.P. Alleviation of the effect of salinity on growth and yield of strawberry by foliar spray of selenium-nanoparticles. *Environ Pollut* **2019**, *253*, 246-258, doi:10.1016/j.envpol.2019.04.078.
7. Christou, A.; Manganaris, G.A.; Papadopoulos, I.; Fotopoulos, V. Hydrogen sulfide induces systemic tolerance to salinity and non-ionic osmotic stress in strawberry plants through modification of reactive species biosynthesis and transcriptional regulation of multiple defence pathways. *J Exp Bot* **2013**, *64*, 1953-1966, doi:10.1093/jxb/ert055.
8. Baral, A. Strawberries under salt stress: ALA and ROS to the rescue. *Physiol Plant* **2019**, *167*, 2-4, doi:10.1111/ppl.13010.

 doi:10.20944/preprints202602.1825.v1

9. Galli, V.; Messias, R.S.; Guzman, F.; Perin, E.C.; Margis, R.; Rombaldi, C.V. Transcriptome analysis of strawberry (Fragaria x ananassa) fruits under osmotic stresses and identification of genes related to ascorbic acid pathway. *Physiol Plant* **2019**, *166*, 979-995, doi:10.1111/ppl.12861.
10. Rizwan, M.; Ali, S.; Ibrahim, M.; Farid, M.; Adrees, M.; Bharwana, S.A.; Zia-Ur-Rehman, M.; Qayyum, M.F.; Abbas, F. Mechanisms of silicon-mediated alleviation of drought and salt stress in plants: a review. *Environ Sci Pollut Res Int* **2015**, *22*, 15416-15431, doi:10.1007/s11356-015-5305-x.
11. Rios, J.J.; Martinez-Ballesta, M.C.; Ruiz, J.M.; Blasco, B.; Carvajal, M. Silicon-mediated Improvement in Plant Salinity Tolerance: The Role of Aquaporins. *Front Plant Sci* **2017**, *8*, 948, doi:10.3389/fpls.2017.00948.
12. Kurowska, M.M. Aquaporins in Cereals-Important Players in Maintaining Cell Homeostasis under Abiotic Stress. *Genes (Basel)* **2021**, *12*, doi:10.3390/genes12040477.
13. Zhu, Y.X.; Xu, X.B.; Hu, Y.H.; Han, W.H.; Yin, J.L.; Li, H.L.; Gong, H.J. Silicon improves salt tolerance by increasing root water uptake in Cucumis sativus L. *Plant Cell Rep* **2015**, *34*, 1629-1646, doi:10.1007/s00299-015-1814-9.
14. Ali, S.; Rizwan, M.; Qayyum, M.F.; Ok, Y.S.; Ibrahim, M.; Riaz, M.; Arif, M.S.; Hafeez, F.; Al-Wabel, M.I.; Shahzad, A.N. Biochar soil amendment on alleviation of drought and salt stress in plants: a critical review. *Environ Sci Pollut Res Int* **2017**, *24*, 12700-12712, doi:10.1007/s11356-017-8904-x.
15. Poveda, J.; Martinez-Gomez, A.; Fenoll, C.; Escobar, C. The Use of Biochar for Plant Pathogen Control. *Phytopathology* **2021**, *111*, 1490-1499, doi:10.1094/PHYTO-06-20-0248-RVW.
16. Berendsen, R.L.; Pieterse, C.M.; Bakker, P.A. The rhizosphere microbiome and plant health. *Trends Plant Sci* **2012**, *17*, 478-486, doi:10.1016/j.tplants.2012.04.001.
17. Edwards, J.; Johnson, C.; Santos-Medellin, C.; Lurie, E.; Podishetty, N.K.; Bhatnagar, S.; Eisen, J.A.; Sundaresan, V. Structure, variation, and assembly of the root-associated microbiomes of rice. *Proc Natl Acad Sci U S A* **2015**, *112*, E911-920, doi:10.1073/pnas.1414592112.
18. Pieterse, C.M.; Zamioudis, C.; Berendsen, R.L.; Weller, D.M.; Van Wees, S.C.; Bakker, P.A. Induced systemic resistance by beneficial microbes. *Annu Rev Phytopathol* **2014**, *52*, 347-375, doi:10.1146/annurev-phyto-082712-102340.
19. Bulgarelli, D.; Schlaeppi, K.; Spaepen, S.; Ver Loren van Themaat, E.; Schulze-Lefert, P. Structure and functions of the bacterial microbiota of plants. *Annu Rev Plant Biol* **2013**, *64*, 807-838, doi:10.1146/annurev-arplant-050312-120106.
20. Souza, R.; Ambrosini, A.; Passaglia, L.M. Plant growth-promoting bacteria as inoculants in agricultural soils. *Genet Mol Biol* **2015**, *38*, 401-419, doi:10.1590/S1415-475738420150053.
21. Glick, B.R. Plant growth-promoting bacteria: mechanisms and applications. *Scientifica (Cairo)* **2012**, *2012*, 963401, doi:10.6064/2012/963401.
22. Orozco-Mosqueda, M.D.C.; Glick, B.R.; Santoyo, G. ACC deaminase in plant growth-promoting bacteria (PGPB): An efficient mechanism to counter salt stress in crops. *Microbiol Res* **2020**, *235*, 126439, doi:10.1016/j.micres.2020.126439.
23. Glick, B.R. Modulation of plant ethylene levels by the bacterial enzyme ACC deaminase. *FEMS Microbiol Lett* **2005**, *251*, 1-7, doi:10.1016/j.femsle.2005.07.030.
24. Glick, B.R. Bacteria with ACC deaminase can promote plant growth and help to feed the world. *Microbiol Res* **2014**, *169*, 30-39, doi:10.1016/j.micres.2013.09.009.
25. Gamalero, E.; Glick, B.R. Recent Advances in Bacterial Amelioration of Plant Drought and Salt Stress. *Biology (Basel)* **2022**, *11*, doi:10.3390/biology11030437.
26. Malik, L.; Sanaullah, M.; Mahmood, F.; Hussain, S.; Siddique, M.H.; Anwar, F.; Shahzad, T. Unlocking the potential of co-applied biochar and plant growth-promoting rhizobacteria (PGPR) for sustainable agriculture under stress conditions. *Chem Biol Technol Agric* **2022**, *9*, 58, doi:10.1186/s40538-022-00327-x.
27. Tu, C.; Wei, J.; Guan, F.; Liu, Y.; Sun, Y.; Luo, Y. Biochar and bacteria inoculated biochar enhanced Cd and Cu immobilization and enzymatic activity in a polluted soil. *Environ Int* **2020**, *137*, 105576, doi:10.1016/j.envint.2020.105576.
28. Bolyen, E.; Rideout, J.R.; Dillon, M.R.; Bokulich, N.A.; Abnet, C.C.; Al-Ghalith, G.A.; Alexander, H.; Alm, E.J.; Arumugam, M.; Asnicar, F.; et al. Reproducible, interactive, scalable and extensible microbiome data science using QIIME 2. *Nat Biotechnol* **2019**, *37*, 852-857, doi:10.1038/s41587-019-0209-9.

 doi:10.20944/preprints202602.1825.v1

29. Callahan, B.J.; McMurdie, P.J.; Rosen, M.J.; Han, A.W.; Johnson, A.J.; Holmes, S.P. DADA2: High-resolution sample inference from Illumina amplicon data. *Nat Methods* **2016**, *13*, 581-583, doi:10.1038/nmeth.3869.
30. Quast, C.; Pruesse, E.; Yilmaz, P.; Gerken, J.; Schweer, T.; Yarza, P.; Peplies, J.; Glockner, F.O. The SILVA ribosomal RNA gene database project: improved data processing and web-based tools. *Nucleic Acids Res* **2013**, *41*, D590-596, doi:10.1093/nar/gks1219.
31. McMurdie, P.J.; Holmes, S. phyloseq: an R package for reproducible interactive analysis and graphics of microbiome census data. *PLoS One* **2013**, *8*, e61217, doi:10.1371/journal.pone.0061217.
32. Lin, H.; Peddada, S.D. Analysis of compositions of microbiomes with bias correction. *Nat Commun* **2020**, *11*, 3514, doi:10.1038/s41467-020-17041-7.
33. Chen, S.; Zhou, Y.; Chen, Y.; Gu, J. fastp: an ultra-fast all-in-one FASTQ preprocessor. *Bioinformatics* **2018**, *34*, i884-i890, doi:10.1093/bioinformatics/bty560.
34. Song, Y.; Peng, Y.; Liu, L.; Li, G.; Zhao, X.; Wang, X.; Cao, S.; Muyle, A.; Zhou, Y.; Zhou, H. Phased gap-free genome assembly of octoploid cultivated strawberry illustrates the genetic and epigenetic divergence among subgenomes. *Hortic Res* **2024**, *11*, uhad252, doi:10.1093/hr/uhad252.
35. Kim, D.; Langmead, B.; Salzberg, S.L. HISAT: a fast spliced aligner with low memory requirements. *Nat Methods* **2015**, *12*, 357-360, doi:10.1038/nmeth.3317.
36. Li, H.; Handsaker, B.; Wysoker, A.; Fennell, T.; Ruan, J.; Homer, N.; Marth, G.; Abecasis, G.; Durbin, R.; Genome Project Data Processing, S. The Sequence Alignment/Map format and SAMtools. *Bioinformatics* **2009**, *25*, 2078-2079, doi:10.1093/bioinformatics/btp352.
37. Pertea, M.; Pertea, G.M.; Antonescu, C.M.; Chang, T.C.; Mendell, J.T.; Salzberg, S.L. StringTie enables improved reconstruction of a transcriptome from RNA-seq reads. *Nat Biotechnol* **2015**, *33*, 290-295, doi:10.1038/nbt.3122.
38. Love, M.I.; Huber, W.; Anders, S. Moderated estimation of fold change and dispersion for RNA-seq data with DESeq2. *Genome Biol* **2014**, *15*, 550, doi:10.1186/s13059-014-0550-8.
39. Chen, C.; Wu, Y.; Li, J.; Wang, X.; Zeng, Z.; Xu, J.; Liu, Y.; Feng, J.; Chen, H.; He, Y.; et al. TBtools-II: A "one for all, all for one" bioinformatics platform for biological big-data mining. *Mol Plant* **2023**, *16*, 1733-1742, doi:10.1016/j.molp.2023.09.010.
40. Hothorn, T.; Bretz, F.; Westfall, P. Simultaneous inference in general parametric models. *Biom J* **2008**, *50*, 346-363, doi:10.1002/bimj.200810425.
41. Hasegawa, P.M.; Bressan, R.A.; Zhu, J.K.; Bohnert, H.J. Plant Cellular and Molecular Responses to High Salinity. *Annu Rev Plant Physiol Plant Mol Biol* **2000**, *51*, 463-499, doi:10.1146/annurev.arplant.51.1.463.
42. Zhu, J.K. Plant salt tolerance. *Trends Plant Sci* **2001**, *6*, 66-71, doi:10.1016/s1360-1385(00)01838-0.
43. Ma, J.F.; Yamaji, N. Silicon uptake and accumulation in higher plants. *Trends Plant Sci* **2006**, *11*, 392-397, doi:10.1016/j.tplants.2006.06.007.
44. Zhu, Y.X.; Gong, H.J.; Yin, J.L. Role of Silicon in Mediating Salt Tolerance in Plants: A Review. *Plants (Basel)* **2019**, *8*, doi:10.3390/plants8060147.
45. Coskun, D.; Deshmukh, R.; Sonah, H.; Menzies, J.G.; Reynolds, O.; Ma, J.F.; Kronzucker, H.J.; Belanger, R.R. The controversies of silicon's role in plant biology. *New Phytol* **2019**, *221*, 67-85, doi:10.1111/nph.15343.
46. Wu, Y.; Wang, X.; Zhang, L.; Zheng, Y.; Liu, X.; Zhang, Y. The critical role of biochar to mitigate the adverse impacts of drought and salinity stress in plants. *Front Plant Sci* **2023**, *14*, 1163451, doi:10.3389/fpls.2023.1163451.
47. Apel, K.; Hirt, H. Reactive oxygen species: metabolism, oxidative stress, and signal transduction. *Annu Rev Plant Biol* **2004**, *55*, 373-399, doi:10.1146/annurev.arplant.55.031903.141701.
48. Foyer, C.H.; Noctor, G. Redox homeostasis and antioxidant signaling: a metabolic interface between stress perception and physiological responses. *Plant Cell* **2005**, *17*, 1866-1875, doi:10.1105/tpc.105.033589.
49. Gill, S.S.; Tuteja, N. Reactive oxygen species and antioxidant machinery in abiotic stress tolerance in crop plants. *Plant Physiol Biochem* **2010**, *48*, 909-930, doi:10.1016/j.plaphy.2010.08.016.
50. Mendes, R.; Garbeva, P.; Raaijmakers, J.M. The rhizosphere microbiome: significance of plant beneficial, plant pathogenic, and human pathogenic microorganisms. *FEMS Microbiol Rev* **2013**, *37*, 634-663, doi:10.1111/1574-6976.12028.

 doi:10.20944/preprints202602.1825.v1

51. Yang, J.; Kloepper, J.W.; Ryu, C.M. Rhizosphere bacteria help plants tolerate abiotic stress. *Trends Plant Sci* **2009**, *14*, 1-4, doi:10.1016/j.tplants.2008.10.004.
52. Etesami, H.; Beattie, G.A. Mining Halophytes for Plant Growth-Promoting Halotolerant Bacteria to Enhance the Salinity Tolerance of Non-halophytic Crops. *Front Microbiol* **2018**, *9*, 148, doi:10.3389/fmicb.2018.00148.